

Electronic Supplementary Information (ESI):

Theoretical analysis of the impact of different
anchoring groups on the efficiency of dye-
sensitized solar cells based on ruthenium

Sepideh Samiee*, Mohadese Ahmadi Manesh

Department of Chemistry, Faculty of Science, Shahid Chamran University of Ahvaz, Ahvaz, Iran

*Corresponding author. Tel: +986133331042; Fax: +986133337009; E-mail address:
s.samiee@scu.ac.ir and samiee.sepideh@gmail.com

Contents	Page
Computational methods.	S3-S5
References	S6-S7
Table S1-S4	S7-S10
Fig. S1-S3	S11-S13

S.1. Computational Methods

SI-1. DFT Calculations

The ground-state geometries of all ruthenium sensitizers were fully optimized in the gas phase and re-optimized in acetonitrile solution using the DFT framework with the B3LYP functional [1,2]. A mixed 6-311+G (d,p) basis set for non-metallic (C, H, O, N, S, P) atoms [30-31] and LANL2DZ basis set for the metal atom Ru [32]), which typically yields excellent results for metal complexes [33,34], was employed in these computations. The optimized geometries are used to calculate the HOMO, LUMO energies, the HOMO and LUMO energy gap (HLG) and to find the frontier molecular orbitals (FMOs) distribution. The nature of the frontier molecular orbitals plays a key role in determining the charge separated states of the dye sensitizers. UV/VIS spectra were included through the TD-DFT approach [3,4], BP86, M06, B3PW91, B3LYP, and CAM-B3LYP functional were tested on ruthenium dye with known absorption spectra. The results clearly indicated that both B3LYP and B3PW91 provided in good agreement with experimental data, but the B3LYP method is less costly compared to the other considered methods (Figure S1 in ESI). It should be note that the effect of the solvent was considered by the polarizable continuum model (PCM) of dichloromethane (CH_2Cl_2). Based on TD-DFT calculations, the light harvesting efficiency (LHE) is also determined for each Ru-dye in both phase and compared with others.

SI-3. Time dependent Density Functional Theory (TD-DFT) Calculations

The light harvesting efficiency (LHE) of the sensitizers affects the overall conversion efficiency (CE) [55]. The LHE is an indicator of the efficiency of converting incident sunlight into electricity. The LHE can be determined using below equation:

$$LHE = 1 - 10^{-f}$$

where f is the oscillator strength of the dye associated with the highest longest wavelength (λ_{\max}). It is recognized that the higher the f value, the higher the LHE value would be. In addition, the performance of DSSCS depends on many parameters such as electron injection ($\Delta G_{\text{inj.}}$), regeneration (ΔG_{reg}), recombination driving force (ΔG_{rec}) and open-circuit photovoltage (V_{oc}), which are obtained from the following Eqs. (1) to (4) [5,6]:

$$\Delta G_{\text{inj.}} = E_{\text{dye}}^* - E_{\text{CB}} \quad (1)$$

where E_{dye}^* is the excited state oxidation potential and E_{CB} is the ground state reduction potential of the semiconductor(TiO_2) in the ground state (-4.0 eV). Herein, E_{dye}^* is calculated by the equation (2):

$$E_{\text{dye}}^* = E_{\text{dye}} - E_{\text{ex}} \quad (2)$$

where E_{dye} is the ground state oxidation potential of the dye , which can be estimated from the negative E_{HOMO} ; E_{ex} is a vertical electronic transition energy related to the longest wavelength. In this context, ΔG_{reg} can be defined by subtracting the oxidation potential of the dye from the oxidation potential of the electrolyte (-4.8 eV):

$$\Delta G_{\text{reg.}} = E_{\text{dye}} - E_{\text{redox}} \quad (3)$$

The open-circuit photovoltage V_{oc} can be calculated as:

$$V_{\text{OC}} = E_{\text{LUMO}} - E_{\text{CB}} \quad (4)$$

The nonlinear optical response (NLO) is related to the photovoltaic properties. It is well known that good dye molecule candidates as DSSCs should have high values of polarizability (α_0) and first-order hyperpolarizability (β_0) [7-10]. Note that the calculated values are in atomic units (a.u.) and are then converted to electrostatic units (esu) (for α_0 : 1 a.u. = 0.1482×10^{-24} esu; for β_0 : 1

a.u.= 0.008639×10^{-30} esu). For each molecule, these parameters are defined by the following equation:

$$\mu_{tot} = \sqrt{\mu_x^2 + \mu_y^2 + \mu_z^2} \quad (5)$$

$$\alpha_0 = \frac{1}{3}(\alpha_{xx} + \alpha_{yy} + \alpha_{zz}) \quad (6)$$

$$\beta_{tot} = [(\beta_{xxx} + \beta_{xyy} + \beta_{zxx})^2 + (\beta_{yyy} + \beta_{yzz} + \beta_{yxz})^2 + (\beta_{zzz} + \beta_{zxz} + \beta_{zyy})^2]^{\frac{1}{2}} \quad (7)$$

References

- [1] C. Lee, W. Yang, G. Parr, Development of the Colle-Salvetti correlation-energy formula into a functional of the electron density, *Phys. Rev. B* 37 (1988) 785–789.
- [2] A. D. Becke, Density-functional exchange-energy approximation with correct asymptotic behavior, *Phys. Rev. A* 38 (1988) 3098–3100.
- [3] R. Sánchez-De-Armas, J. O. López, M. A. San-Miguel, J. F. Sanz, P. Ordejón, M. Pruneda, Real-Time TD-DFT Simulations in Dye Sensitized Solar Cells: The Electronic Absorption Spectrum of Alizarin Supported on TiO₂ Nanoclusters, *J. Chem. Theory Comput.*, 6 (2010) 2856–2865.
- [4] C. Adamo, T. Le Bahers, M. Savarese, L. Wilbraham, G. García, R. Fukuda, M. Ehara, N. Rega, I. Ciofini, Exploring excited states using Time Dependent Density Functional Theory and density-based indexes, *Coord. Chem. Rev.*, 304 (2015) 166–178.
- [5] S. Meng, E. Kaxiras, M. K. Nazeeruddin, M. Gratzel, Design of Dye Acceptors for Photovoltaics from First-Principles Calculations, *J. Phys. Chem. C* 115 (2011) 9276–9282.
- [6] P. Ganesan, A. Yella, T. W. Holcombe, P. Gao, R. Rajalingam, S. A. Al-Muhtaseb, M. Gratzel, M. K. Nazeeruddin, Unravel the impact of anchoring groups on the photovoltaic performances of diketopyrrolopyrrole sensitizers for dye-sensitized solar cells. *ACS Sustain. Chem. Eng.*, 3 (2015) 2389–2396.
- [7] M.-M. Chen, H.-G. Xue, S.-P. Guo, Multinary metal chalcogenides with tetrahedral structures for second-order nonlinear optical, photocatalytic, and photovoltaic applications, *Coord. Chem. Rev.* 368 (2018) 115–133.

- [8] F. Meyers, S. R. Marder, B. M. Pierce, J. Bredas, Electric field modulated nonlinear optical properties of Donor-Acceptor polyenes: Sum-Over-States investigation of the relationship between molecular Polarizabilities (.alpha., .beta., and .gamma.) and bond length alternation, *J. Am. Chem. Soc.* 116 (1994) 10703–10714.
- [9] N. H. List, R. Zales'ny, N. A. Murugan, J. Kongsted, W. Bartkowiak, H. Agren, Relation between nonlinear optical properties of push–pull molecules and metric of charge transfer excitations, *J. Chem. Theory Comput.* 11 (2015) 4182–4188.
- [10] S. J. Sharma, N. Sekar, Charge Transfer as Bridging Correlator for DSSC Efficiency and NLO Property, *Chem. Select.* 7 (2022) e202203262.

Table S1. The optimized main geometry parameters for all considered Ru(II) dyes in gas phase

Ref. dye	Ru-dye 1	Ru-dye 2	Ru-dye 3	Ru-dye 4	Ru-dye 5	Ru-dye 6	Ru-dye 7	Ru-dye 8	Ru-dye 9	Ru-dye 10	Ru-dye 11	
Bond lengths												
Ru–N(1) ^a	2.067	2.070	2.077	2.093	2.068	2.059	2.060	2.087	2.048	2.103	2.057	2.064
Ru–N(2)	2.067	2.070	2.077	2.093	2.070	2.058	2.063	2.086	2.048	2.068	2.066	2.062
Ru–N(3) ^b	2.086	2.086	2.092	2.086	2.087	2.081	2.082	2.079	2.079	2.068	2.077	2.092
Ru–N(4)	2.091	2.091	2.098	2.088	2.093	2.084	2.084	2.080	2.086	2.070	2.090	2.103
Ru–N(5)	2.091	2.091	2.098	2.088	2.089	2.084	2.083	2.080	2.086	2.089	2.085	2.102
Ru–N(6)	2.086	2.086	2.092	2.086	2.086	2.080	2.081	2.079	2.079	2.110	2.081	2.091
N=C	1.184	1.184	1.183	1.186	1.183	1.185	1.185	1.187	1.187	1.183	1.188	1.183
C=S	1.632	1.633	1.637	1.634	1.633	1.627	1.628	1.629	1.621	1.640	1.624	1.633
Bond angles												
N(1)–Ru–N(4)	172.69	172.61	172.75	173.84	172.54	172.63	172.70	173.79	172.56	172.93	172.48	172.42
N(2)–Ru–N(5)	172.69	172.61	172.75	173.84	172.38	172.80	172.82	173.79	172.56	175.58	172.48	172.60
N(3)–Ru–N(6)	177.88	177.61	177.46	179.90	177.38	177.94	177.94	179.40	178.72	177.09	178.99	177.65
N(5)–Ru–N(6)	78.16	77.95	77.61	77.82	77.97	78.45	78.38	78.42	78.50	78.80	78.38	78.91
N(2)–Ru–N(3)	86.91	86.96	86.56	83.91	87.24	86.92	86.84	84.20	86.82	80.40	86.73	87.76
N(1)–Ru–N(5)	86.44	86.29	85.80	83.84	86.22	86.85	86.67	84.711	87.11	85.92	88.02	86.35

Table S2. The optimized main geometry parameters for all considered Ru(II) dyes in solvent (ACN) phase

Ref. dye	Ru-dye 1	Ru-dye 2	Ru-dye 3	Ru-dye 4	Ru-dye 5	Ru-dye 6	Ru-dye 7	Ru-dye 8	Ru-dye 9	Ru-dye 10	Ru-dye 11	
Bond lengths												
Ru–N(1) ^a	2.067	2.070	2.077	2.093	2.068	2.059	2.060	2.087	2.048	2.103	2.057	2.064
Ru–N(2)	2.067	2.070	2.077	2.093	2.070	2.058	2.063	2.086	2.048	2.068	2.066	2.062
Ru–N(3) ^b	2.086	2.086	2.092	2.086	2.087	2.081	2.082	2.079	2.079	2.068	2.077	2.092
Ru–N(4)	2.091	2.091	2.098	2.088	2.093	2.084	2.084	2.080	2.086	2.070	2.090	2.103
Ru–N(5)	2.091	2.091	2.098	2.088	2.089	2.084	2.083	2.080	2.086	2.089	2.085	2.102
Ru–N(6)	2.086	2.086	2.092	2.086	2.086	2.080	2.081	2.079	2.079	2.110	2.081	2.091
N=C	1.184	1.184	1.183	1.186	1.183	1.185	1.185	1.187	1.187	1.183	1.188	1.183
C=S	1.632	1.633	1.637	1.634	1.633	1.627	1.628	1.629	1.621	1.640	1.624	1.633
Bond angles												
N(1)–Ru–N(4)	172.69	172.61	172.76	173.84	172.54	172.63	172.70	173.79	172.57	172.94	172.49	172.43
N(2)–Ru–N(5)	172.69	172.61	172.76	173.85	172.39	172.80	172.81	173.80	172.56	175.57	172.48	172.61
N(3)–Ru–N(6)	177.88	177.616	177.47	179.91	177.38	177.95	177.94	179.40	178.72	177.09	178.99	177.65
N(5)–Ru–N(6)	78.16	77.96	77.614	77.82	77.97	78.45	78.38	78.42	78.50	78.80	78.39	78.92
N(2)–Ru–N(3)	86.91	86.96	86.56	83.91	87.24	86.93	86.84	84.20	86.82	80.40	86.73	87.76
N(1)–Ru–N(5)	86.45	86.29	85.81	83.85	86.23	86.85	86.67	84.72	87.12	85.92	88.02	86.35

Table S3. Comparison of selected calculated bond lengths (Å) and angles (°) for three desired Ru-dyes with experimental values from X-ray analysis.

Bond lengths	Ref. dye	Ru-dye 1	Ru-dye 8	Exp.[41]	Exp.[42]
Ru–N(1) ^a	2.067	2.070	2.048	–	2.044
Ru–N(2)	2.067	2.070	2.048	2.055	2.050
Ru–N(3) ^b	2.086	2.086	2.079	2.051	2.026
Ru–N(4)	2.091	2.091	2.086	2.041	2.042
Ru–N(5)	2.091	2.091	2.086	–	2.026
Ru–N(6)	2.086	2.086	2.079	–	2.062
N=C	1.184	1.184	1.187	1.124	1.156
C=S	1.632	1.633	1.621	1.654	1.642
Bond angles					
N(1)–Ru–N(4)	172.69	172.61	172.56	–	171.81
N(2)–Ru–N(5)	172.69	172.61	172.56	175.82	175.65
N(3)–Ru–N(6)	177.88	177.61	178.72	173.03	176.90
N(5)–Ru–N(6)	78.16	77.95	78.50	–	79.04
N(2)–Ru–N(3)	86.91	86.96	86.82	87.82	88.86
N(1)–Ru–N(5)	86.44	86.29	87.11	–	88.71

Table S4. Calculated absorption wavelength (λ_{abs} in nm), vertical excitation energies (E_{ex} in eV), oscillator strength (f) and light-harvesting efficiency (LHE) for the studied Ru-dyes in gas phase.

	λ_{abs}	E_{ex}	f	LHE	Nature of transitions
Ref. dye	330	3.75	0.0062	0.014	H→L+6 (50%), H→L+9 (27%)
	417	2.97	0.1069	0.218	H-6→L (75%), H-5→L+1 (11%)
	665	1.86	0.0226	0.050	H-3→L+1 (97%) H→L (2%)
Ru-dye 1	325	3.81	0.0106	0.024	H-6→L+2 (37%), H-5→L+3 (14%)
	421	2.93	0.0617	0.132	H-6→L (55%), H-3→L+3 (31%)
	744	1.66	0.0151	0.034	H-2→L+1 (96%) H→L(2%)
Ru-dye 2	325	3.80	0.0163	0.036	H-6→L+2 (31%), H-1→L+8 (15%)
	423	2.92	0.0558	0.120	H-6→L (76%), H-5→LUMO (10%)
	687	1.80	0.0167	0.037	H-2→L+1 (93%)
Ru-dye 3	329	3.75	0.0194	0.043	H-6→L+2 (25%), H-4→L+3 (57%)
	418	2.96	0.0881	0.183	H-6→L+1 (80%), H-5→L+1 (11%)
	656	1.88	0.0405	0.089	H-2→L (75%), H-1→L+1 (17%)
Ru-dye 4	327	3.78	0.0167	0.037	H-6→L+2(52%),H→L+7 (24%)
	422	2.93	0.0731	0.154	H-6→L (56%), H-3→L+4 (24%)
	734	1.68	0.0173	0.039	H-2→L+1 (80%),
Ru-dye 5	371	3.33	0.0824	0.172	H-4→L+2 (39%), H→L+9 (32%)
	443	2.79	0.1707	0.325	H-6→L (71%), H-5→L+1 (18%)
	688	1.79	0.0426	0.093	H→L+3 (86%)
Ru-dye 6	368	3.36	0.1306	0.259	H-5→L+3 (18%), H-4→L+2 (56%)
	440	2.81	0.1895	0.353	H-6→L(72%), H-5→L+1 (17%)
	691	1.79	0.0392	0.086	H→L+2 (88%)
Ru-dye 7	360	3.44	0.077	0.162	H-5→L+2 (83%) H-6→L+2 (8%)
	427	2.90	0.15	0.292	H-6→L+1 (76%), H-5→L+1 (10%)
	734	1.68	0.0399	0.087	H-2→L (76%)
Ru-dye 8	416	2.97	0.1478	0.288	H-5→L+3 (64%), H-4→L+2 (25%)
	908	1.36	0.0629	0.134	H-3→L+2 (12%), H→L+3 (56%)
Ru-dye 9	337	3.67	0.0897	0.186	H-4→L+3 (29%), H-4→L+4 (20%)
	405	3.05	0.0972	0.200	H-6→L (49%), H-6→L+1 (21%)
	530	2.33	0.0373	0.082	H-1→L+3 (19%),H→L+4 (48%)
	772	1.60	0.0357	0.078	H→L+1 (82%)
Ru-dye 10	344	3.60	0.0413	0.090	H-5→L+4 (13%), H-4→L+4 (32%)
	440	2.81	0.1581	0.305	H-6→L (73%), H-5→L+1 (16%)
	777	1.59	0.0334	0.074	H-3→L+1 (86%)
Ru-dye 11	418	2.9	0.1119	0.227	H-6→L (71%), H-5→L+1 (5%)
	656	1.88	0.0203	0.045	H-3→L+1 (87%) H-3→L+4 (5%)

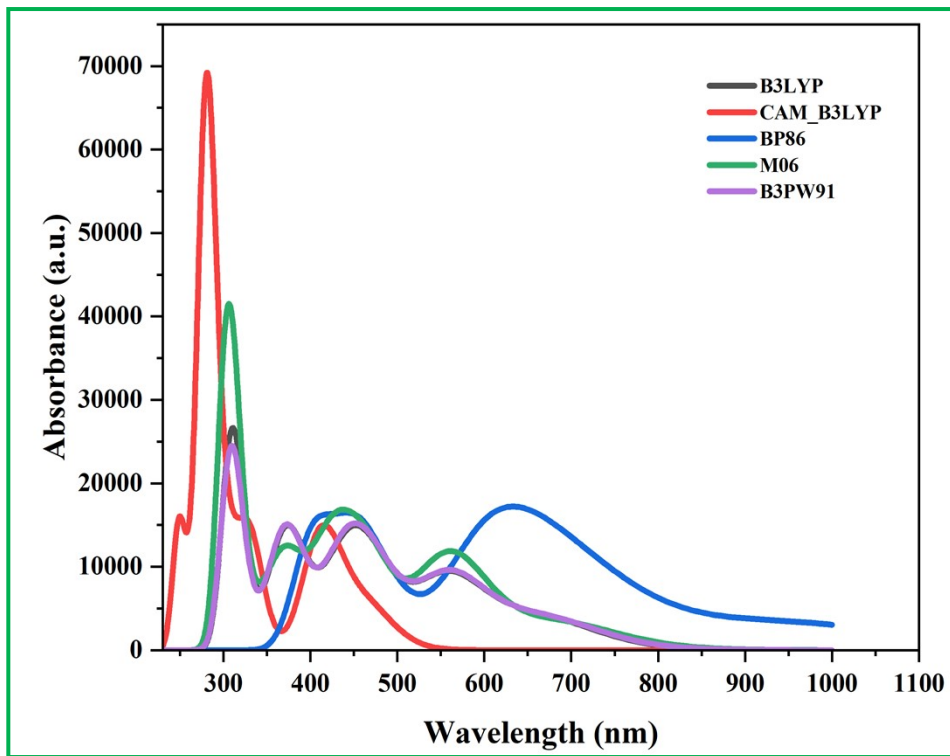


Figure S1. A comparison between the performances of density functional methods for **Ru-dye 5** investigated here.

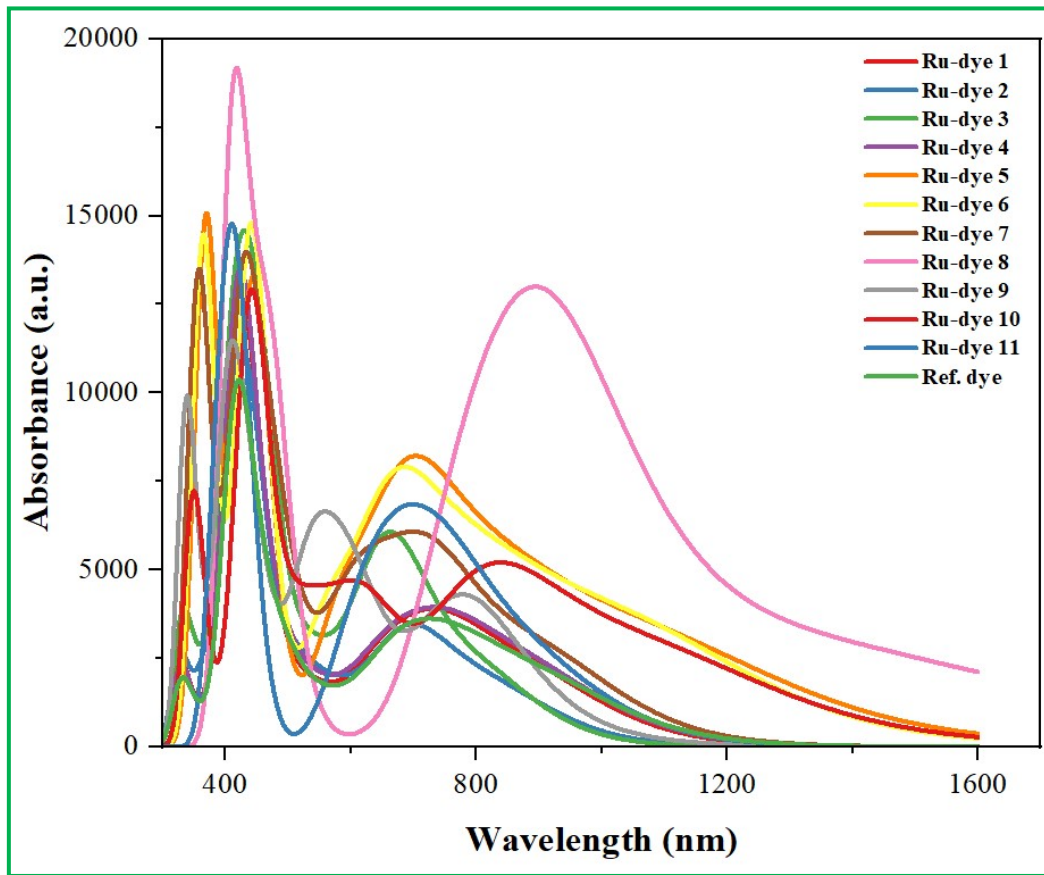


Figure S2. Theoretical UV–vis spectra for all Ru-dyes and the reference dye $[\text{Ru}(\text{bpy})_2(\text{NCS})_2]$; All simulations are obtained using the B3LYP/6–311+G(d,p)/LANL2DZ model in vacuum.

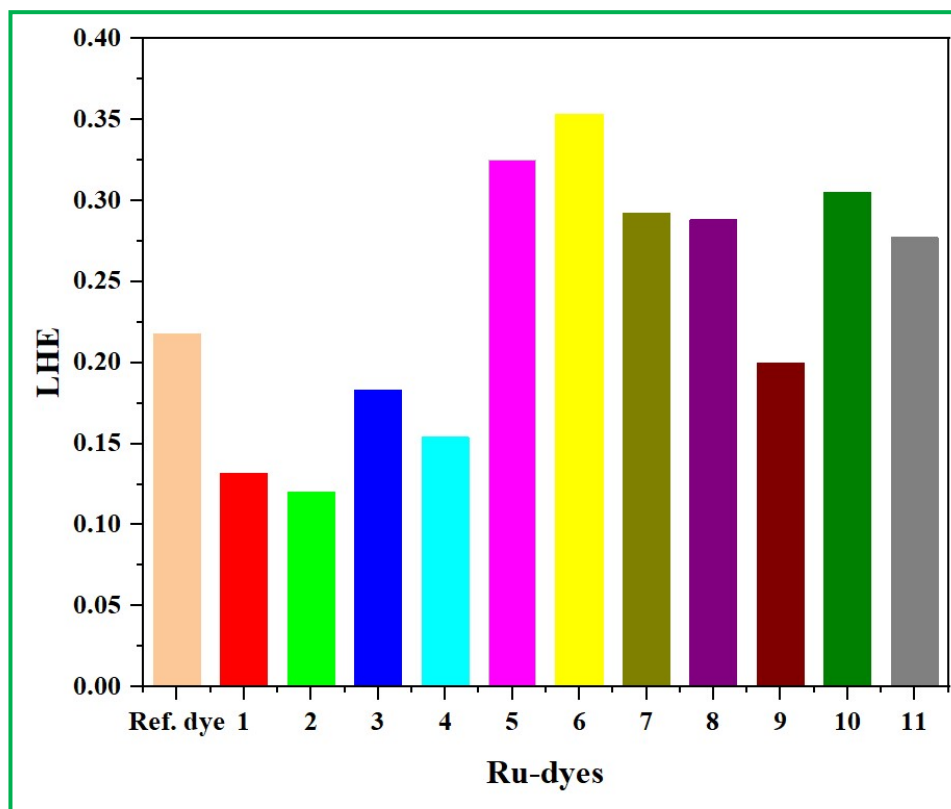


Figure S3. Comparison among the light-harvesting efficiency (LHE) of the **Ru-dyes** (1–11) with the reference dye in acetonitrile solvent.